

Lattice Response of Quantum Solids to an Impulsive Local Perturbation

L. Bonacina, P. Larrégaray, F. van Mourik, and M. Chergui*

Laboratoire de Spectroscopie Ultrarapide, ISIC, FSB-BSP, Ecole Polytechnique Fédérale de Lausanne, CH-1015 Lausanne, Switzerland[†]

(Received 23 March 2005; published 1 July 2005)

The lattice response of solid para-H₂ to an impulsive electronic excitation was studied using femto-second pump-probe spectroscopy. The evolution of an electronic bubble in the crystal, created upon excitation of the $A(3s\sigma)$ Rydberg state of an NO impurity, was followed in real time, with a resolution of 100 fs. The experimental results, interpreted in connection with molecular dynamics simulations with quantum corrections, indicate the presence of three stages in the dynamics: a sub-100 fs “adiabatic” phase, a 0.5–1 ps phase, corresponding to the interaction of the first with the next shells driven by the bubble expansion, and a 5 ps phase, corresponding to a slow rearrangement of the environment surrounding the impurity. These findings indicate that the lattice response in solid para-H₂ resembles that of a liquid.

DOI: 10.1103/PhysRevLett.95.015301

PACS numbers: 67.80.Cx, 78.47.+p

Solid Hydrogen has been attracting attention not only as the simplest molecular crystal [1,2], but also as a quantum crystal [3]. Its most distinctive quantum aspect is the large amplitude of zero-point (ZP) lattice vibrations, amounting to $\sim 20\%$ of the intermolecular distance, which affects most properties of the solid. The potential use of solid para-H₂ doped with small atomic impurities as a propellant has motivated a series of optical spectroscopic studies [4,5], and theoretical simulations based on path integral methods [6–9], which are aimed at providing a molecular level description of the photoinduced dynamics and energy dissipation. Quantum effects have mainly been investigated by steady-state spectroscopic methods, in particular, high-resolution spectroscopy [10–12]. A more direct insight is provided by time-domain experiments, using ultrashort pulse excitation of the atomic or molecular impurity embedded in the H₂ lattice. Ideally, the excitation should create an impulsive perturbation leading to considerable conformational changes, which one can probe in real time. Our approach is based on the excitation of a dopant molecule, NO, to its lowest Rydberg state, $A(3s\sigma)$ [13]. Because of the strong repulsive interaction of the extended Rydberg orbital with the surrounding H₂ molecules, the absorption band is strongly blue shifted (by ~ 0.6 eV) with respect to the gas phase. Fluorescence is strongly Stokes shifted, occurring at nearly the gas phase energy [13], which suggests the occurrence of an extensive local structural rearrangement, known as a “bubble” formation, well documented in other media such as rare gas liquids and solids [14,15]. In a simple configuration coordinate (in fact, the cage radius) model, we estimated [13] the size of the bubble to be ~ 5 Å, i.e., 25–30% larger than the ground state NO-H₂ distance, almost doubling the volume it occupies. Bubbles also occur around electrons [16–18] or atomic impurities excited to Rydberg states [5] in solid H₂ or D₂. Electron bubbles in solid H₂ were detected using IR spectroscopy [16–18], and their radius estimated to

~ 5 Å. The path integral Monte Carlo simulations on Li-doped solid para-H₂ showed a similar Li-H₂ distance for single substitutional sites [6,7,19]. These simulations also showed that the defects heal very quickly away from the impurity. In none of these studies was the time scale for the rearrangement of the lattice estimated. Note that the ground state of Li, characterized by a lone unpaired s electron, resembles a Rydberg orbital. In our previous femtosecond experiments on NO-doped solid normal-H₂ and normal-D₂ [20], we estimated the time scale for bubble formation to ≤ 300 fs, slightly below the time resolution of that experiment (~ 350 fs). Here, using an improved time resolution of ~ 100 fs, we unravel hitherto unobserved details of the bubble expansion and energy dissipation mechanisms in NO-doped solid para-H₂, which are

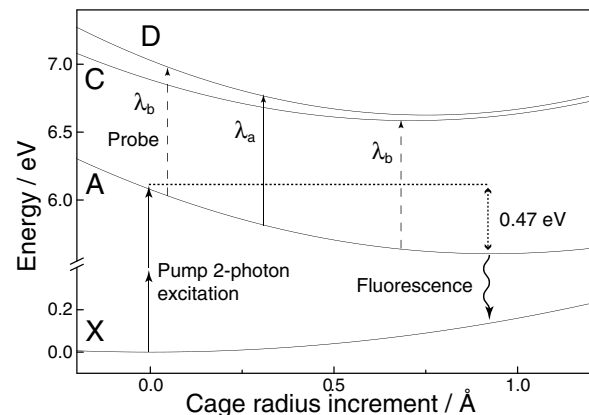


FIG. 1. Potential energy curves of the NO-matrix cage interaction in solid H₂, as a function of the cage radius increment [13]. The pump pulse excites the A state by 2-photon absorption. The dynamics of bubble formation is probed inducing transitions from the A to the C or D states, and detecting the depletion of the $A \rightarrow X$ fluorescence. Depending on the probe wavelengths, only one (λ_a) or two (λ_b) probe windows are opened.

supported by classical molecular dynamics (MD) simulations with quantum corrections.

The principle of the experiment has been described elsewhere [20]. It is presented in Fig. 1, which shows the intermolecular NO-matrix cage potentials for the ground state and the lowest three Rydberg states of NO in solid H₂, which we derived from the analysis of the spectroscopic line shapes [13].

Contrary to the one-photon excitation used in Ref. [20], here the pump pulse excites the (*A*(3s σ)) state of NO in solid para-H₂ by 2-photon absorption at 400 nm. This reaches the *A*-state potential at an excess energy of ~ 0.47 eV above its minimum, which is the energy that drives the bubble formation. Probe pulses between ~ 1.4 and $\sim 1.1 \mu\text{m}$ are used to follow the dynamics on the *A* state, by inducing transitions to the next higher *C* and *D* Rydberg states. The detected signal is the depletion of the (long-lived) fluorescence of the *A* state as a function of pump-probe time delay. Indeed, the population that is transferred by the probe pulse from *A* to *C* or *D*, does not come back to the *A* state [21]. Since the intermolecular

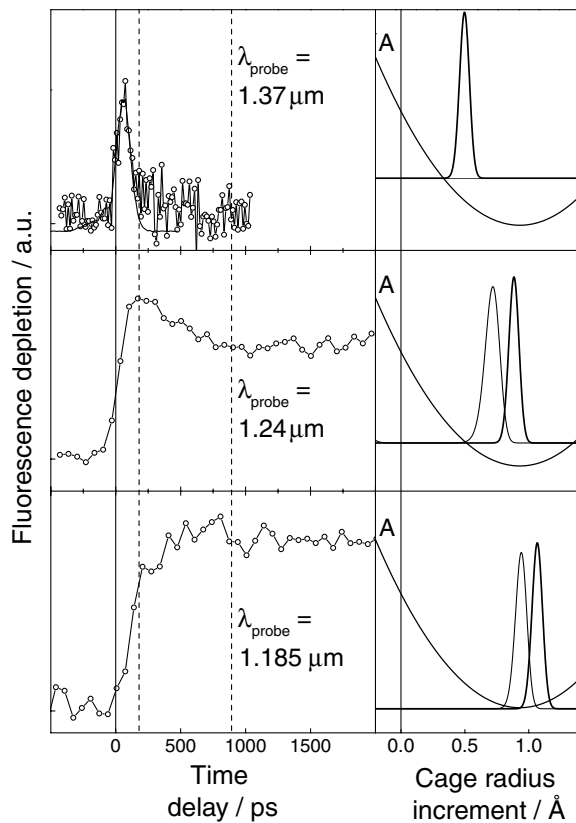


FIG. 2. Left: Pump-probe transient scans for different probe wavelengths. The vertical dashed lines represent the onset of the different dynamical regimes described in the text (see also Fig. 4). Right: *A*-*C* (thick line) and *A*-*D* (thin line) probe windows corresponding to the different probe wavelengths along the *A*-state potential.

A-*C* and *A*-*D* difference potentials vary along the deformation coordinate (bubble radius), the different λ_{probe} 's sample distinct configurations of the bubble (see Fig. 2, right panels). It is important to stress that our experiment directly visualizes the motion of the first shell around the impurity, imparted by excitation of the latter. Time zero and the cross-correlation of ~ 100 fs between pump and probe pulses, are determined *in situ* by difference frequency mixing at the surface of the sample. The doped crystal is prepared by condensing a mixture of para-H₂ with NO at a partial pressure of 0.2% onto a CaF₂ window cooled to 3.5 K.

Figure 2 shows typical pump-probe transients (left panels) of the first ps, corresponding to probe windows (right panels) at different stages of the dynamics. The bluest wavelength ($1.185 \mu\text{m}$) samples the arrival of the population in the relaxed final configuration. Therefore the signal has a step-function-like character. However, it exhibits a bimodal rise with a prompt ~ 200 fs, followed by a slower 600–700 fs component (see dashed vertical lines). On the other hand, transients measured using the reddest probe wavelength ($1.37 \mu\text{m}$), which samples a midway configuration, show a single peak, reflecting the passage of the dynamics at this configuration. The peak maximum lies at ~ 100 fs time delay. Interestingly, it has the same width as the cross-correlation of our experiment, pointing to a coherent expansion of the bubble up to this point, in the sense that all excited sites respond in a synchronous fashion. In addition, by then, up to $\sim 50\%$ of the excess potential energy available for bubble expansion has been dissipated. Together with the $1.185 \mu\text{m}$ transient, this suggests that the first sub-200 fs step represents an energy release of over 50%, while the rest is dissipated during the subsequent 600–700 fs. The intermediate transient at $1.24 \mu\text{m}$ reflects the probing of the dynamics at the two configurations, indicated in the right panel. The first window samples the

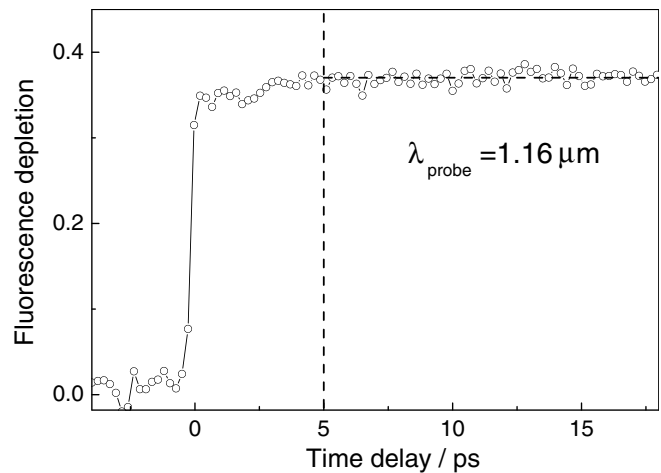


FIG. 3. Long time pump-probe transient at the blue most probe wavelength. The dashed line indicates the long time evolution of the signal.

passage of the dynamics at a later time than for the $1.37 \mu\text{m}$ probe: it causes the steep rise of the first structure, which indeed peaks at a later time (see dashed vertical line) than at $1.37 \mu\text{m}$. The second window samples the final configuration, and the signal indeed reflects the buildup of the population, causing the persistence of a depletion signal at longer times.

Figure 3 shows that dynamics still goes on at $t \geq 1$ ps. Indeed, there is a further rise of the signal on a ~ 5 ps time scale. This rise shows up better at the bluest probe wavelengths, and suggests a further conformational rearrangement following the sub-ps bubble expansion. The levelling off of the signal beyond ~ 5 ps (dashed vertical line) indicates that after this time delay the system has fully relaxed [20].

The significance of these various time regimes becomes clearer in the light of our MD simulations. We resort to a classical approach, in view of the lack of simulations methods of the ultrafast dynamics in condensed phase quantum media (see Ref. [22] for a review). In order to mimic the ZP fluctuations, we raise the temperature at which the simulations are run. This is the basis of the thermal harmonic quantum correction [23], which consists of treating the nuclear motion of the system as harmonic oscillations, and correcting the temperature at which the classical calculations are performed. The effective temperature is chosen in such a way that the classical probability distribution equals the quantum one at the real temperature. This choice is determined by the Debye frequency of the solid. However, this is not applicable in the case of a highly anharmonic solid such as solid H_2 . We therefore selected the temperature by simulating the radial distribution function (RDF) of the neat solid that best reproduces that obtained by path integral Monte Carlo simulations [6]. This leads to an effective temperature of

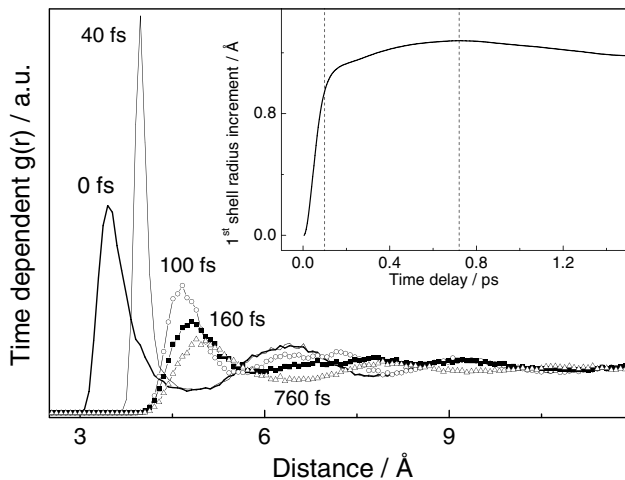


FIG. 4. Simulations of the time-dependent radial distribution function around NO for different delays after excitation. Inset: Radius increment of the 1st shell of H_2 molecules around the NO impurity as a function of time.

20 K. The simulations were carried out in a box of 800 para- H_2 molecules and one NO impurity. Isotropic intermolecular H_2 - H_2 potentials [24] were used. For the NO- H_2 ground state potential, we used the experimentally determined NO-Ne potential [25], after noting that the construction of the potential by combination rules yielded a very similar result [26]. Finally the NO* A - H_2 potential was generated by simulating, using equilibrium MD, the steady-state absorption and emission of the NO A state in solid H_2 to get the best agreement with the experimental ones [13]. The lattice response dynamics was simulated using non equilibrium MD consisting of an average of 2000 trajectories. More details will be given in a forthcoming publication [27]. Figure 4 shows snapshots of the RDF around the impurity at different time delays, while the inset shows the radius increment of the first shell (to which our experiment is sensitive). Soon after excitation (40 fs), the RDF shows a sharp focussing of the spatial distribution of the first shell molecules, which confirms the coherent nature of the expansion at early times, as evidenced by the width of the signal at $\lambda_{\text{probe}} = 1.37 \mu\text{m}$ (Fig. 2). For $t < 100$ fs, the second and higher shells are silent, suggesting that no energy exchange has yet taken place between the first and the next shells. Therefore, the expansion is an adiabatic process, even though the experimental results suggest that more than 50% of the excess potential energy has been released. The trajectory of the first shell radius (inset) shows that during this time $\sim 80\%$ of the expansion takes place, confirming our analysis of the $1.37 \mu\text{m}$ transient. The adiabatic character of the initial expansion stage was also observed in the case of bubble formation in solid Argon [28]. At $t \approx 100$ fs, the higher shells start to move, while the first shell merges into the second, leading to a slowing down of the bubble expansion, especially at $t > 150$ fs (inset). This phase lasts up to ~ 700 fs, in very good agreement with the conclusion from the experimental data. Finally, our simulations also show a rearrangement over longer times (not shown here), in that the area of the first and second peaks in the RDF of the relaxed lattice slightly changes between 750 fs and the limit of our simulations (a few ps), in line with the results of Fig. 3. At the same time, we see that the next shells reorder with an internuclear distance close to that of the solid before excitation. Thus, the rapid healing of structural defects away from the impurity, which was reported in the path integral simulations on Li-doped solid H_2 [6], already occurs at the second shell, on a time scale of 5 ps.

The above results represent the first detailed account of structural dynamics in a quantum solid. Contrary to conventional solids, which upon impulsive excitation exhibit coherent oscillations due to localized modes [28–31], the behavior reported here is closer to that found in liquids, where the solvent rearrangement is characterized by three time scales [32,33]. The first (< 100 fs) is associated with the rapid relaxation resulting from the free motions of the

molecules within the potential wells they initially occupy. This relaxation is reversible (adiabatic), in the sense that each individual molecule evolves freely, without dissipation. In the present case, this regime corresponds to the sudden expansion of the first shell, before any energy exchange with the rest of the lattice occurs. Following this sharp break in the response, the solvent begins to restructure itself, and energy irreversibly flows into the medium, such that the regime is now dissipative, with time scales between 0.5 and 4 ps [33]. In the present context, this corresponds to the second stage, lasting ~ 0.7 ps where the first shell merges with the next. In most solvents, a third response appears that can take up to tens of ps, which is due to larger amplitude motions around the probe. This corresponds to the 5 ps reorganization of the lattice shells observed here. Thus it appears that, on these short time scales, solid H_2 behaves like a liquid rather than a solid. Nevertheless, the hydrodynamic model which we previously implemented [20,34] cannot adequately describe the multiple time scales characterizing the dynamics. The response we find has to do with the delocalized character of the solid species, and with its strongly anharmonic nature. Given the scarcity of studies on condensed quantum media, the present results offer an ideal benchmark for developing tools to simulate their ultrafast dynamics.

This work was supported by the Swiss NSF via Grants No. 2000-061897.00 and No. 2000-67912.02.

*Electronic address: majed.chergui@epfl.ch

†URL: <http://lsu.epfl.ch/>

- [1] I. F. Silvera, *Rev. Mod. Phys.* **52**, 393 (1980).
- [2] J. van Kranendonk, *Solid Hydrogen* (Plenum Press, New York, 1983).
- [3] L. H. Nosanow, *Phys. Rev.* **146**, 120 (1966).
- [4] M. E. Fajardo, S. Tam, T. L. Thompson, and M. E. Cordonnier, *Chem. Phys.* **189**, 351 (1994).
- [5] S. Tam, M. Macler, M. E. DeRose, and M. E. Fajardo, *J. Chem. Phys.* **113**, 9067 (2000).
- [6] D. Scharf, G. J. Martyna, D. H. Li, G. A. Voth, and M. L. Klein, *J. Chem. Phys.* **99**, 9013 (1993).
- [7] E. Cheng and K. B. Whaley, *J. Chem. Phys.* **104**, 3155 (1996).
- [8] J. R. Krumrine, S. M. Jang, M. H. Alexander, and G. A. Voth, *J. Chem. Phys.* **113**, 9079 (2000).
- [9] Y. M. Ma, T. Cui, and G. T. Zou, *J. Chem. Phys.* **114**, 3092 (2001).
- [10] T. Oka, *Annu. Rev. Phys. Chem.* **44**, 299 (1993).
- [11] H. Katsuki, M. Fushitani, and T. Momose, *Low Temp. Phys.* **29**, 832 (2003).
- [12] H. Katsuki and T. Momose, *Phys. Rev. Lett.* **84**, 3286 (2000).
- [13] F. Vigliotti, A. Cavina, C. Bressler, B. Lang, and M. Chergui, *J. Chem. Phys.* **116**, 4542 (2002).
- [14] M. Chergui, N. Schwentner, and V. Chandrasekharan, *J. Chem. Phys.* **89**, 1277 (1988).
- [15] N. Schwentner, E. Koch, and J. Jortner, *Electronic Excitations of Condensed Rare Gases* (Springer, Berlin, 1985).
- [16] S. K. Bose and J. D. Poll, *Can. J. Phys.* **63**, 1105 (1985).
- [17] R. L. Brooks, S. K. Bose, J. L. Hunt, J. R. Macdonald, J. D. Poll, and J. C. Waddington, *Phys. Rev. B* **32**, 2478 (1985).
- [18] S. K. Bose and J. D. Poll, *Can. J. Phys.* **63**, 94 (1985).
- [19] T. Cui, Y. Takada, Q. Cui, Y. Ma, and G. Zou, *Phys. Rev. B* **64**, 024108 (2001).
- [20] F. Vigliotti, L. Bonacina, and M. Chergui, *J. Chem. Phys.* **116**, 4553 (2002).
- [21] F. Vigliotti, M. Chergui, M. Dickgiesser, and N. Schwentner, *Faraday Discuss.* **108** 139 (1997).
- [22] G. Rojas-Lorenzo, J. Rubayo-Soneira, F. Vigliotti, and M. Chergui, *Phys. Rev. B* **67**, 115119 (2003).
- [23] J. P. Bergsma, P. H. Berens, K. R. Wilson, D. R. Fredkin, and E. J. Heller, *J. Phys. Chem.* **88**, 612 (1984).
- [24] I. F. Silvera and V. V. Goldman, *J. Chem. Phys.* **69**, 4209 (1978).
- [25] H. Thuis, S. Stolte, and J. Reuss, *Chem. Phys.* **43**, 351 (1979).
- [26] H. M. Lin, M. Seaver, K. Y. Tang, A. E. W. Knight, and C. S. Parmenter, *J. Chem. Phys.* **70**, 5442 (1979).
- [27] L. Bonacina, P. Larrégaray, F. van Mourik, and M. Chergui (to be published).
- [28] C. Jeannin, M. T. PortellaOberli, S. Jimenez, F. Vigliotti, B. Lang, and M. Chergui, *Chem. Phys. Lett.* **316**, 51 (2000).
- [29] M. Nisoli, S. DeSilvestri, O. Svelto, R. Scholz, R. Fanciulli, V. Pellegrini, F. Beltram, and F. Bassani, *Phys. Rev. Lett.* **77**, 3463 (1996).
- [30] L. Dhar, J. A. Rogers, and K. A. Nelson, *Chem. Rev.* **94**, 157 (1994).
- [31] T. Tokizaki, T. Makimura, H. Akiyama, A. Nakamura, K. Tanimura, and N. Itoh, *Phys. Rev. Lett.* **67**, 2701 (1991).
- [32] R. Jimenez, G. R. Fleming, P. V. Kumar, and M. Maroncelli, *Nature (London)* **369**, 471 (1994).
- [33] M. L. Horng, J. A. Gardecki, A. Papazyan, and M. Maroncelli, *J. Phys. Chem.* **99**, 17311 (1995).
- [34] F. Vigliotti, E. Sarraf, M. Chergui, and R. Scholz, *Phys. Rev. Lett.* **83**, 2355 (1999).